Closely coupled superconducting microbridges

H. J. T. Smith and M. Dion
Guelph-Waterloo Program for Graduate Work in Physics, Waterloo Campus, University of Waterloo, Ontario, Canada N2L 3G1
(Received 15 February 1990)

Two closely coupled superconducting microbridges have been fabricated with the length of the separating superconducting region less than a coherence length. These microbridges exhibit coupling even when there is zero bias potential at each microbridge. The critical current of each microbridge is a function of the bias current of the other microbridge. This type of coupling is explained by a coupling current that is proportional to the sine of the sum of the phases of both microbridges.

INTRODUCTION

Many workers have extensively studied the interactions that occur between superconducting microbridges where the coupling is not strong. Bindslev-Hansen and Lindelof[1] have written an extensive review. When the separation of two microbridges is less than the coherence length, order-parameter interactions can occur. The order-parameter depression due to one microbridge occurs at the location of the other and vice versa. Such an interaction can occur at zero and nonzero potentials.

Interactions between microbridges due to nonequilibrium quasiparticles occur when the microbridge separation is less than the quasiparticle charge imbalance length and when there is a potential across at least one microbridge. The nonequilibrium state of the quasiparticles at a microbridge is caused by the potential across it. These nonequilibrium states do not decay but diffuse to the other microbridge.

In this paper, experimental data is presented of the coupling between two microbridges separated by a distance that is much less than the coherence A model based on pair coupling between the extreme regions of the two microbridges is used to explain this data.

THEORY

Suppose that two superconducting microbridges [Fig. 1(a)] are separated by a distance, which is much less than the coherence length, and assume that the microbridges have a planar structure. The phases of each of the microbridges will be a function of the potential and current of both microbridges. The magnitude of a Josephson tunnel current is a function of both the barrier and the superconducting state in each of the two adjacent regions. In this model the length of the superconducting region B between the two microbridges is less than the coherence length and this will cause the Josephson tunnel current of each microbridge to be reduced from the value they would have if the center region were of infinite dimension. At the same time because the region B is small there is a probability of pair tunneling between region A and region C. Thus the source current I_1 in the absence of potentials at either microbridge, is a sum of two parts, the tunnel current between regions A and B plus a pair tunnel current between region A and region C. Similarly the source current, I_2 is a sum of the tunnel current between regions B and C and a tunnel current between regions A and C. The pair tunnel current between regions A and C gives rise to a coupling of the phase of the two microbridges. The equivalent circuit of this model is represented in Fig. 1(b).

$$I_{1,2}=I_{c1,c2}\sin(\phi_{1,2})+\beta\sin(\phi_1+\phi_2)\ , \tag{1}$$

where $I_{c1,c2}$ are the critical currents of the two microbridges in the absence of coupling. $\phi_{1,2}$ are the phases of each of the microbridges and β is a parameter that represents the strength of the tunnel current between regions A and C. Combining Eq. (1) with the resistively shunted junction model gives the following time-dependent phase relations:

$$\frac{\hbar}{2eR_{1,2}}\frac{d\phi_{1,2}}{dt}=I_{1,2}-I_{c1,c2}\sin(\phi_{1,2})-\beta\sin(\phi_1+\phi_2)\ , \tag{2}$$

where $R_{1,2}$ are the normal-state resistances of the micro-

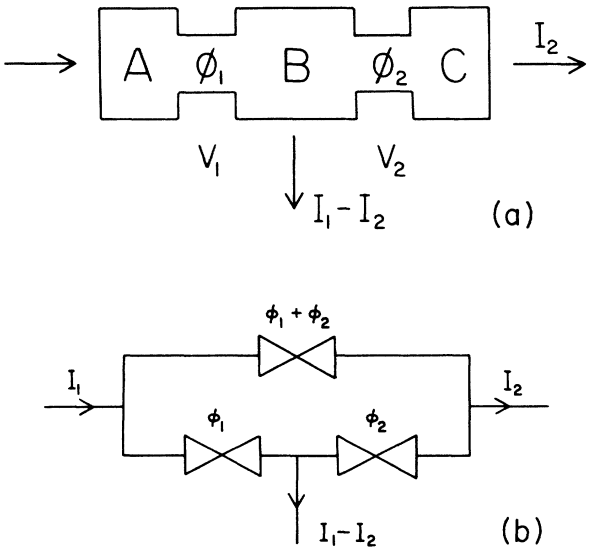

FIG. 1. (a) Ideal geometry of the coupled microbridges. (b) The equivalent circuit of the coupled microbridges from which Eq. (1) was derived.

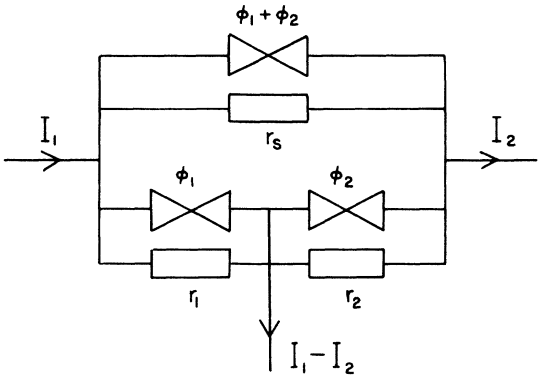

FIG. 2. A more complete equivalent circuit for this model which includes both the junction shunt resistors as well as the quasiparticle current coupling.

bridges. The potentials of the microbridges are given by

$$V_{1,2}=\frac{\hbar d\phi_{1,2}}{2edt} . \tag{3}$$

At finite potentials quasiparticle coupling will also be present and it can be incorporated into Eq. (2) by adding a term that is proportional to the potential of the other microbridge:[2]

$$\frac{\hbar}{2eR_{1,2}}\frac{d\phi_{1,2}}{dt}=I_{1,2}-I_{c1,c2}\sin(\phi_{1,2}) -\beta(1-\alpha_{1,2})\sin(\phi_1+\phi_2) -\alpha_{1,2}[I_{2,1}-I_{c2,c1}\sin(\phi_{2,1})] . \tag{4}$$

The factors $\alpha_{1,2}$ are dependent on the strength of the quasiparticle coupling. Figure 2 is a more complete equivalent circuit of Eq. (4), but note that there is not a direct equivalence between the actual junction shunt resistors of the actual model and the equivalent circuit because the quasiparticle coupling current is proportional to the potential across the opposite microbridge. The following equivalences should be noted:

$$\alpha_{1,2}=\frac{r_{1,2}}{r_{1,2}+r_s} , \tag{5}$$

$$R_{1,2}=\frac{r_{1,2}(r_{2,1}+r_s)}{r_1+r_2+r_s} . \tag{6}$$

EXPERIMENT

In order to test Eq. (4), two closely coupled tin microbridges were fabricated by a technique that has been previously described.[3] In this paper two samples of coupled microbridges are discussed. In sample No. 1 the length of the microbridges and the thickness of the outside banks were 0.3 μm. The separation of the microbridges was 0.2 μm. The diameter of the microbridges was approximately 1.0 μm. The current-voltage characteristics of one microbridge was monitored while a fixed bias was maintained on the other. Measurements were made close to T_c in order that there be no hysteresis in the current-

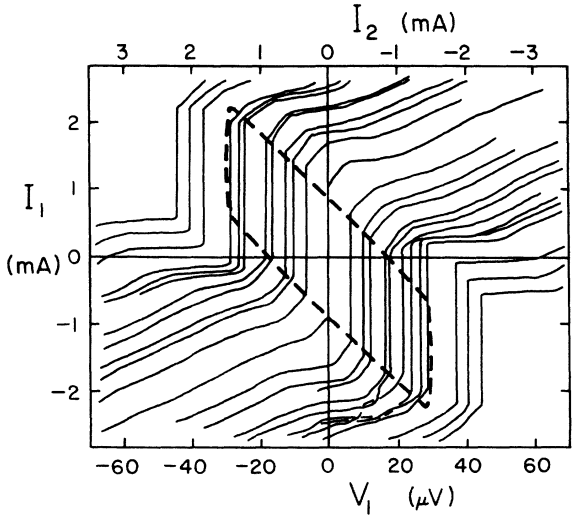

FIG. 3. Current-voltage (I_1-V_1) characteristics of microbridge 1 at $T/T_c=0.978$ for different values of I_2. The curves have been shifted horizontally by the magnitude of I_2. The dashed line is a map of the critical current of microbridge 1 as a function of I_2 for $\beta=1.42$ mA, $I_{c2}=0.81$ mA, $I_{c2}=0.08$ mA and zero potential across microbridge 2.

voltage characteristic, and in these calculations the capacitances of the microbridges has been omitted. Furthermore, close to T_c the coherence length is increased and for these films at this temperature it is of the order 1 μm (Fig. 3), is a series of current-voltage characteristics (I_1-V_1) at $T/T_c=0.978$. For convenience each of the curves has been displaced horizontally by an amount equal to the fixed bias current through microbridge 2. In Fig. 3 the potential of microbridge 2 is zero for the current range -1.2 mA $< I_2 < 1.2$ mA. Figure 4 is a series of current-voltage characteristics (V_2-I_2) at the same tem-

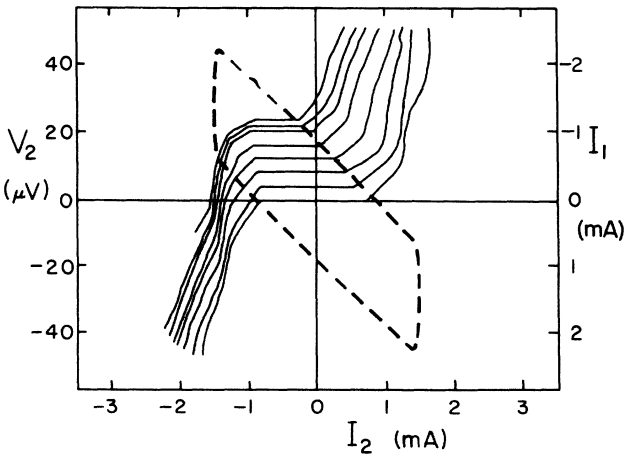

FIG. 4. Voltage-current (V_2-I_2) characteristic of microbridge 2 at $T/T_c=0.978$ for different values of I_1. The curves have been shifted vertically by the magnitude of I_1. The dashed line is a map of the critical current of microbridge 2 as a function of I_1 for $\beta=1.42$ mA, $I_{c1}=0.81$ mA, $I_{c2}=0.08$ mA, and zero potential across microbridge 1.

perature. For convenience each of the curves has been displaced vertically by an amount equal to the fixed bias current through microbridge 1. The experimental plots of Figs. 3 and 4 show a region in the vicinity of the origin where the potentials of both microbridges are zero. In this region the critical current of microbridge 1 is a function of the current I_2 through microbridge 2 even though there is no potential across microbridge 2. In similar fashion the critical current of microbridge 2 is a function of the current I_1 even though there is no potential across microbridge 1. Such a change of critical current cannot be explained by quasiparticle coupling but it can be explained by the model described in this paper. Order-parameter coupling can give rise to two effects; first, there is the depression of the order parameter at one microbridge due to the current through the other and secondly, when the separation of the microbridges is less than the coherence length the phase of each microbridge will be altered by the current through the other. Way *et al.*[4] reported that a pair of double microbridges will behave as one when the separating region is less then a coherence length. Depression of the order parameter has been discussed by Lindelof and Bindslev-Hansen[5] and it has been observed by Jillie, Lukens, and Kao.[6] They found that when a supercurrent was passed through microbridge 2 the critical current of microbridge 1 was depressed regardless of the current direction. The separation of their microbridges was 2.0 μm.

In the experiments that are reported in this paper the separation of the microbridges was 0.2 μm and when a current was passed through microbridge 2, the critical current of microbridge 1 was either increased or decreased according to the current direction through microbridge 1. We suggest that this behavior may be explained by the model outlined in this paper where the phases of the microbridges are coupled. The condition for maximum zero-voltage currents in both microbridges can be obtained from Eq. (2) and it is given by

$$\beta\cos(\phi_1+\phi_2)[I_{c1}\cos(\phi_1)+I_{c2}\cos(\phi_2)] + I_{c1}\cos(\phi_1)I_{c2}\cos(\phi_2)=0\ . \quad (7)$$

Equation (7) has been solved numerically and the parameters I_{c1}, I_{c2}, and β were adjusted to give the best fit to the critical currents of Figs. 3 and 4. The parameter values are $\beta=1.42$ mA, $I_{c1}=0.81$ mA, and $I_{c2}=0.08$ mA. The map of the critical current of microbridge 2 as a function of I_1 and the map of the critical current of microbridge 1 as a function of I_2 are indicated by dash lines in Figs. 3 and 4. Whilst there is not complete quantitative agreement between the dashed line and the critical current values, they do follow the same general trend. The critical current of each microbridge is strongly dependent on the current through the other microbridge. The experimental data of Figs. 3 and 4 show a similar behavior for the critical currents in the range -1.2 mA $< I_2 < 1.2$ mA. Thus this type of coupling gives a shift in the critical current of one microbridge proportional to the current of the other microbridge, even though the potential of the other microbridge is zero. This is an effect that nonequilibrium quasiparticle coupling cannot predict. It is interesting to compare some experimental current-voltage curves to similar curves calculated from Eq. (4).

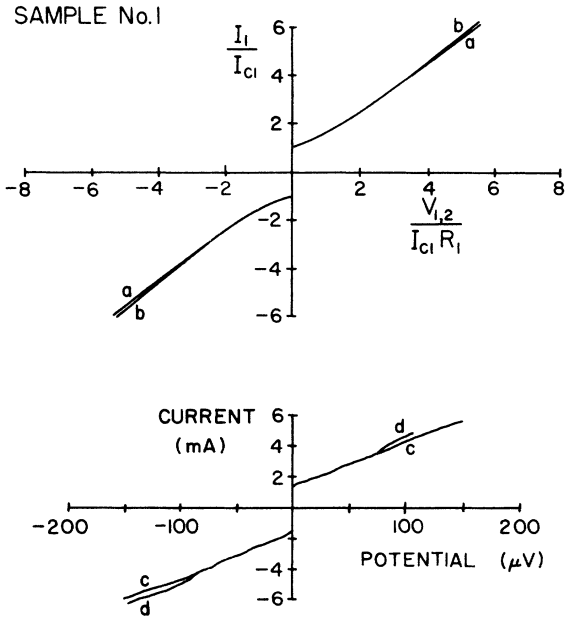

FIG. 5. Calculations of (*a*) I_1-V_1 and (*b*) I_1-V_2 with $\alpha_{1,2}=0.405$ mA, $\beta=1.42$ mA, $I_2=0$, $I_{c1}=0.81$ mA, $I_{c2}=0.08$ mA, $R_1=0.025\ \Omega$, and $R_2=0.039\ \Omega$. Experimental curves (*c*) I_1-V_1 and (*d*) I_1-V_2 with $I_2=0$ and $T/T_c=0.978$.

Curves (*a*) and (*b*) of Fig. 5 were calculated from Eq. (4) using estimates of $\alpha_{1,2}=0.405$ mA, $\beta=1.42$ mA, $I_{c1}=0.81$ mA, $I_{c2}=0.08$ mA, $R_1=0.025\ \Omega$, and $R_2=0.039\ \Omega$ for the case of $I_2=0$. Curves (*c*) and (*d*) of Fig. 5 are the corresponding experimental data for (I_1-

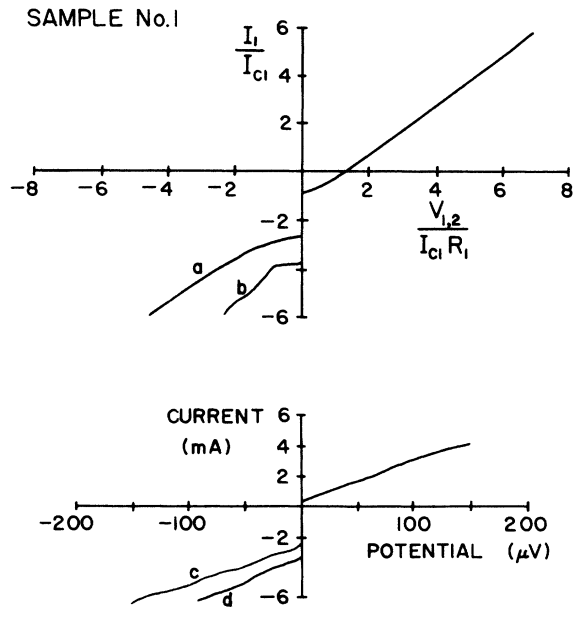

FIG. 6. Same as Fig. 5 but with a theoretical value of $I_2=-1.46$ mA, and an experimental value of $I_2=-0.89$ mA.

V_1) and (I_1-V_2) with $I_2=0$ for the coupled microbridges at $T/T_c=0.978$. Voltage locking, at low potentials, is present in both the theoretical and the experimental plots. Figure 6 is the same as Fig. 5 with the exception that $I_2=-1.46$ mA for the calculation and $I_2=-0.89$ mA in the experiment. The magnitude of I_2 was adjusted for the calculated curves until they were similar to the experimental data. Once again, both the theoretical and experimental plots show voltage locking. In Fig. 7, I_2 has been decreased to -1.62 mA for the calculation and -1.27 mA for the experiment so that V_2 is not coincidentally zero when V_1 is zero. Note that both the experimental and theoretical plots show curvature of the I_1-V_1 plot when V_1 is zero. The phase coupling term $\sin(\phi_1+\phi_2)$ of Eq. (4) is essential to produce voltage locking at low potentials and a shift of the critical current. Although there is qualitative agreement between the theory and experiment, we must keep in mind that a number of parameters such as the microbridge capacitance have not been included in these calculations. Also nonequilibrium quasiparticles at each microbridge give rise to a dynamically enhanced critical current or "foot" as it is often termed. This "foot" has been discussed by Schmid, Schon, and Tinkham.[7] In Figs. 3 and 4 the "foot" is present, and it is modified by the potential of the other microbridge, with the result that it masks to some extent the coupling discussed in this paper.

Voltage locking at low potentials in coupled indium microbridges has been reported by Shi *et al.*[8] and by Dai, Yeh, and Kao.[9] In their work on closely spaced microbridges, Neumann, Dai, and Kao[10] observed voltage locking at currents just greater than the apparent critical current. Jillie *et al.*[11] fabricated Josephson junctions separated by about a coherence length. They observed that the critical currents were synchronized and that the potentials of the two junctions were pulled together and synchronized over a range of currents greater than the critical current. Deminova and Kovalenko[12] have calculated, using an approximate Ginzburg-Landau equation, the effect of the coupling between two strongly coupled microbridges. They found regions of voltage locking and showed that the critical current should decrease with the increase of the coupling. This is in contrast with our experimental data.

The model that has been described in this paper was further tested by applying it to a second sample of coupled microbridges whose phase coupling is weaker than that of sample No. 1. In sample No. 2 the length of the microbridges was 0.1 μm and the thickness of the tin layer separating them was 0.2 μm. The thickness of the banks was 0.3 μm. Current-voltage characteristics were measured at $T/T_c=0.964$ and calculations of current-voltage characteristics were made using Eq. (4) and the parameter values $\alpha_{1,2}=1.08$ mA, $\beta=1.08$ mA, $I_{c1}=4.0$ mA, $I_{c2}=0.2$ mA, $R_1=0.020$ Ω, $R_2=0.048$ Ω, and $I_2=0$. In Fig. 8 curves (*a*) and (*b*) are theoretical plots of (I_1-V_1) and (I_1-V_2) and curves (*c*) and (*d*) are experimental data of (I_1-V_1) and (I_1-V_2). Figure 9 is the same as Fig. 8 with the exception that $I_2=-1.4$ mA for the calculation and $I_2=-0.8$ mA for the experiment. The value of I_2 that was used in the calculation was found by adjusting it until the theoretical and experimental current-voltage curves were similar.

One feature that is present in both the theoretical and

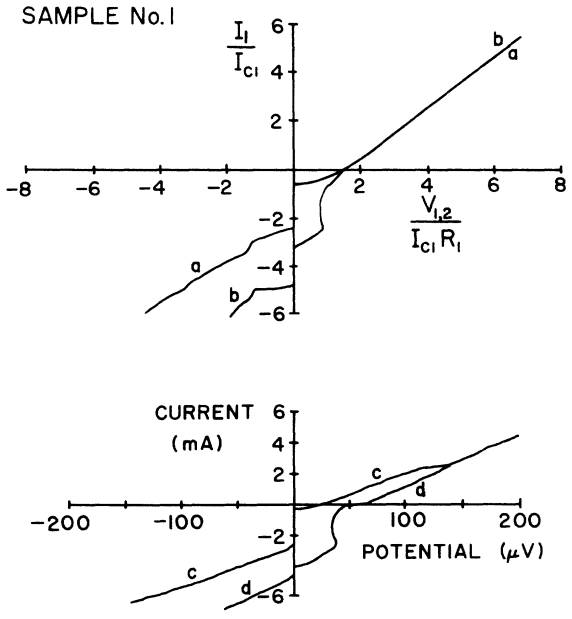

FIG. 7. Same as Fig. 5 but with a theoretical value of $I_2=-1.62$ mA, and an experimental value of $I_2=-1.27$ mA.

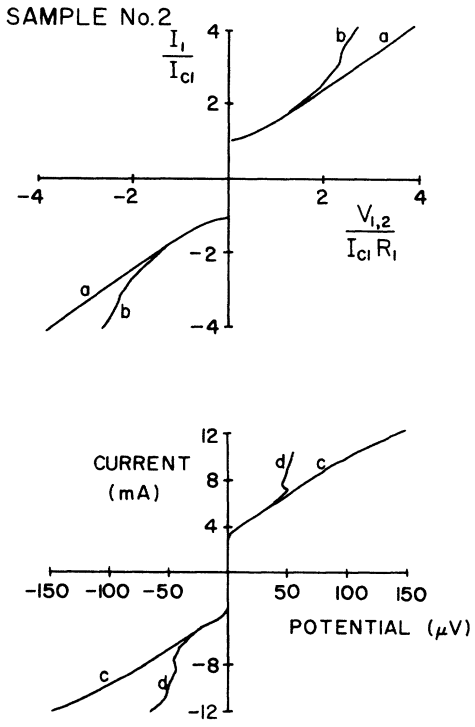

FIG. 8. Calculation of (*a*) I_1-V_1 and (*b*) I_1-V_2 with $\alpha_{1,2}=1.08$ mA, $\beta=1.08$ mA, $I_{c1}=4.0$ mA, $I_{c2}=0.2$ mA, $R_1=0.02$, Ω, $R_2=0.048$ Ω, and $I_2=0$. Experimental curves (*c*) I_1-V_1 and (*d*) I_1-V_2 with $I_2=0$ and $T/T_c=0.964$.

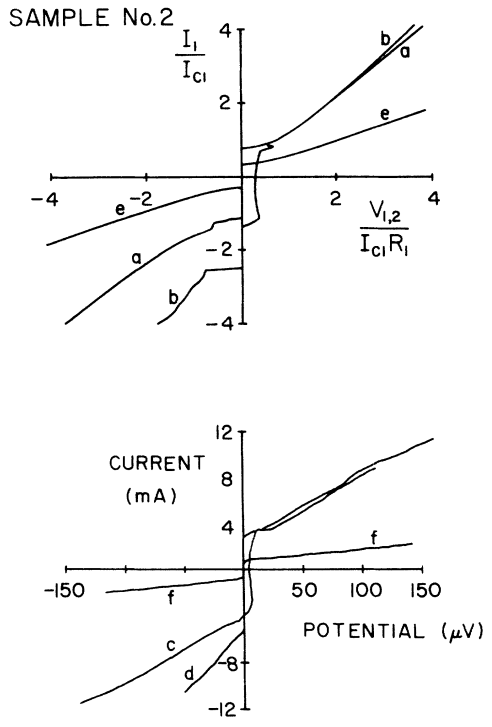

FIG. 9. Same as Fig. 8 but with a theoretical value of $I_2=-1.4$ mA and an experimental value of $I_2=-0.8$ mA. Curve (e) is a theoretical plot of I_2-V_2 for $I_1=0$ and (f) is the corresponding experimental plot.

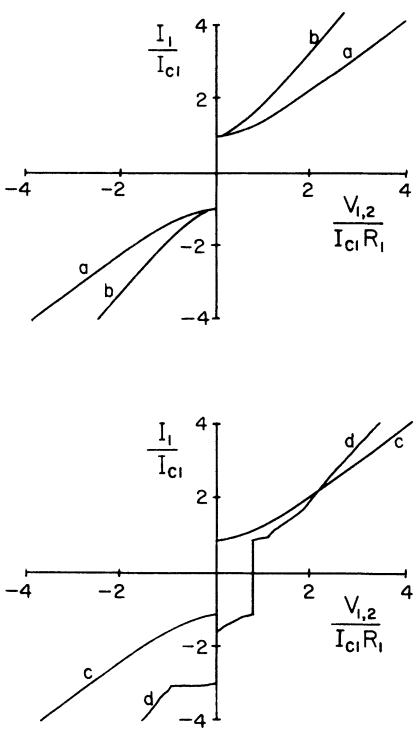

FIG. 10. Curves (a) and (b) were calculated with the same parameters used to calculate curves (a) and (b) of Fig. 8 but with $\beta=0$. Curves (c) and (d) were calculated with the same parameters as Fig. 9 with the exception of $\beta=0$.

experimental data of samples Nos. 1 and 2 is the locking of the potentials of the two microbridges at a value of I_1 just greater than the critical current when $I_2=0$. In order to show that the phase coupling term is responsible for the locking, Eq. (4) was solved numerically with $\beta=0$ and the same parameters as were used in Fig. 8. The result, plotted in Fig. 10, clearly shows that the voltage locking has disappeared.

A second feature that is present in both the experimental theoretical data of samples Nos. 1 and 2 is the curvature of the (I_1-V_2) characteristic when $V_1=0$. In order to illustrate that the phase coupling term is responsible for this feature, Eq. (4) was solved numerically with $\beta=0$ and with all other parameters having the same values that were used when calculating curves (a) and (b) of Fig. 9. The results of these calculations are curves (c) and (d) of Fig. 10. The curvature in the (I_1-V_2) plot when $V_1=0$ is absent. Other workers have observed (I_1-V_2) characteristics of coupled microbridges with similar curvature at low currents. Neumann, Dai, and Kao[10] have measured the current-voltage characteristics of closely spaced superconducting weak links which had been fabricated using standard electron beam lithography techniques. In the inset of Fig. 1 of Ref. 10 they report an (I_1-V_2) characteristic curve for values of the current I_1 that is less than the critical current of weak link 1. They attribute this curvature to a changing ac impedance of weak link 1. Shi *et al.*[8] have reported measurements on a four terminal network of four superconducting weak links. Their current-voltage characteristics (Fig. 3 of Ref. 8) exhibits curvature of the characteristic at low currents.

The coupling $\beta/I_{c1}=1.75$ of sample No. 1 was greater than the coupling $\beta/I_{c1}=0.27$ of sample No. 2, and consequently the shift of the critical current as a function of I_2 of sample No. 2 was much less than for sample No. 1. For the same reason the critical currents of microbridges 1 and 2 of sample No. 1 are almost equal when current through the other microbridge is zero, and for sample No. 2 the critical currents are different [curve (c) of Fig. 8 and curve (f) of Fig. 9].

CONCLUSION

We have shown that quasiparticle coupling is not sufficient to explain the current-voltage characteristics of closely coupled microbridges at zero potentials. The inclusion of a phase coupling term proportional to the sum of the phases of the two microbridges in the equation of motion of the coupled microbridges is necessary to explain qualitatively the experimental data. Three main features of the experimental data are (i) the increase or decrease of the critical current of one microbridge depending on the current through the other microbridge even with no potential across the second microbridge; (ii) the voltage locking at low currents with $I_2=0$; and (iii) the curvature of the I_1-V_2 characteristic when V_1 is zero. A simple model based on a tunnel current between the

two outermost banks of the pair of microbridges will generate a coupling term that is proportional to the sine of the sum of the phases of the two microbridges. This model demonstrates the three main features of the current-voltage characteristics that are experimentally observed.

ACKNOWLEDGMENTS

The authors would like to acknowledge useful discussions with J. A. Blackburn. This work was supported in part by a grant from the Natural Science and Engineering Research Council of Canada.

[1]J. Bindslev-Hansen and P. E. Lindelof, Rev. Mod. Phys. **56**, 431 (1984).

[2]D. W. Jillie, M. A. H. Nerenberg, and J. A. Blackburn, Phys. Rev. B **21**, 125 (1980).

[3]R. Escudero and H. J. T. Smith, J. Appl. Phys. **56**, 3271 (1984).

[4]Y. S. Way, K. S. Hsu, and Y. H. Kao, Phys. Rev. Lett. **39**, 1684 (1977).

[5]P. E. Lindelof and J. Bindslev-Hansen, *Nonequilibrium Superconductivity Phonons and Kapitz Boundaries,* edited by K. E. Gray (Plenum, New York, 1981).

[6]D. W. Jillie, J. E. Lukens, and Y. H. Kao, Phys. Rev. Lett. **38**, 915 (1977).

[7]A. Schmid. G. Schon, and M. Tinkham, Phys. Rev. B **21**, 5076 (1980).

[8]Bao-Yi Shi, Lide Zhang, Yuang-Dong Dai, and Y. H. Kao, J. Low Temp. Phys. **54**, 519 (1984).

[9]Yuan-Dong Dai, W. J. Yeh, and Y. H. Kao, J. Low Temp. Phys. **48** 373 (1982).

[10]L. G. Neumann, Y. D. Dai, and Y. H. Kao, Appl. Phys. Lett. **39**, 648 (1981).

[11]D. W. Jillie, J. E. Lukens, Y. H. Kao, and G. J. Dolan, Phys. Lett. **55A**, 381 (1976).

[12]G. F. Deminova and A. S. Kovelanko, IEEE Trans. Magn. **MAG-15**, 291 (1979).